3

Nonlinear Control Applied to the Rheology of Drops in Elongational Flows with Vorticity

Israel Y. Rosas[1], Marco A. H. Reyes[2], A. A. Minzoni[3] and E. Geffroy[1]
[1]*Instituto de Investigaciones en Materiales,*
[2]*Facultad de Ingeniería,*
[3]*Instituto de Investigaciones en Matemáticas Aplicadas y Sistemas*
Universidad Nacional Autónoma de México, Mexico City
Mexico

1. Introduction

Fluid systems where a liquid phase is dispersed in other liquid, as emulsions, are present in many industrial processes, technological applications and in natural systems. The flow of these substances shows a rheological behavior that depends on the viscosities ratio, the surface tension, surfactants, flow-type parameter and the coupled effects of the fluid structure and the kinematics properties of the flow, mainly in the non linear regimen, which is the reason because the dynamics of the fluid particles is an area of current research. As an approach to understand the physical properties of these fluids, studies on the deformation, break-up and coalescence of drops have been performed since the pioneering work of Taylor (1932).

The deformation and breakup of liquid drops is dependent on the kinematics properties of the imposed flow, in particular of the second invariant of the rate of deformation tensor II_{2D} and the flow-type parameter, α (see Astarita, 1979). In experimental studies of the dynamics, break-up and coalescence of drops, then it is necessary to be able to modify on demand the external flow field parameters causing the drop deformation. For example, Taylor (1934) use two flow devices, a Parallel Band Apparatus (PBA) and a Four-Roll Mill (FRM), which manually manipulated each of the rollers speeds to position a drop. Once the drop was in place, Taylor was able to track changes that occur on the drop shape as a function of the imposed flow, although for a short time, until the drop was ejected from its unstable position.

Four-Roll Mills and Parallel Band cover a wide interval in the flow-type parameter; however, there is a gap between them that the flow fields generated by co-rotating Two-Roll Mill (TRM) geometries fill. PBA works for simple shear flow, corresponding to a flow-type parameter $\alpha = 0$; FRM setup is more effective in the interval $0.4 \leq \alpha \leq 1$ [Yang *et al.* (2001)], whereas TRM is effective in the interval $0.03 \leq \alpha \leq 0.3$ [Reyes and Geffroy (2000b)].

In the case of the Four-Roll Mill, Bentley and Leal (1986a) have shown how to control -for long times- the position of drops within the flow field generated by a FRM by adjusting with a computer and in real-time the speed of rotation of each cylinder, and maintaining

simultaneously constant values for the elongational flow field parameters. This is achieved by modifying the angular velocity of the cylinders, which displaces the stagnation point to a new position, in order to drive the motion of the drop along the stable flow direction towards the stagnation point. Leal's research group at the Chemical Engineering Department at UC Santa Barbara had worked since that with the FRM apparatus, mainly in the pure elongational flow regimen. In the case of the Parallel Band Apparatus, Birkhoffer (2005) proposes computer-controlled flow cell based on the PBA using a digital proportional-integral-differential controller.

We present a nonlinear control applied to study the rheology of a drop in an elongational flow field with vorticity. Large deformations on fluid particles such as drops occur typically in regions containing saddle points. However, the kinematics of a saddle-point flow does not allow for long observation times of the deformed drop due to the outgoing streamlines, which advect the drop away from the flow region of interest. Thus, it is necessary to accurately control the centroid of the drop to study its desired rheology. A suitable control mechanism is essential to maintain the drop position under known flow conditions for times that are long compared to the intrinsic time scales of the dynamics.

In this work, the control mechanism of the position of a drop around the stagnation point of the flow generated by a co-rotating Two-Roll Mill is presented. This control is based on the Poincaré-Bendixson theorem for two-dimensional ordinary differential equations. Namely, when a particle moves within a closed region containing a saddle point inside and the vector field of the equation points inwards at the boundary of the region, the particle undergoes a stable attractive periodic motion. We show that given a prescribed tolerance region, around the unstable stagnation point, an incoming flow can always be generated when the center of mass of the drop reaches the boundary of the tolerance region. This perturbed flow is produced by adjusting the angular velocity of the cylinders, calculated using an analytical solution for the flow, without significant change in the flow parameters. This gives the time dependent analogue of the Poincaré-Bendixson situation just described. The drop is controlled in a perturbed attracting periodic trajectory around the saddle point, while being confined to a prescribed tolerance area. This mechanism is very different from the one used for the proportional control which modifies the unstable nature of the saddle point by adjusting the angular velocities of the cylinder to project the motion along the stable direction only. In the proposed control the effect of the unstable direction combined with the flow readjustment produces the periodic motion.

A nonlinear control strategy, based on the Poincaré-Bendixson theory, is proposed and studied. In essence, the control generates the planar motion of a particle (the centroid in this case) to ensure a periodic motion of the drop centroid inside a prescribed area around the saddle point. In addition, a numerical study and an experimental situation are presented to illustrate the effect of the control on the drop motion. The implementation of the nonlinear control is within a closed region containing the saddle point, with the velocity field pointing inward at every point on the boundary, while the particle undergoes a stable attractive periodic motion. Thus, given a prescribed tolerance region around the stagnation point, it is always possible to generate a controlled incoming flow whenever the center of mass of the liquid drop reaches the boundary of the tolerance region to force the centroid back into the prescribed tolerance region.

The proposed control scheme is capable of keeping the values of the global flow parameters within a small tolerance, and redirecting the liquid-drop centroid toward the stagnation point on a time scale that is much shorter than that of the evolution, with minimal impact upon the liquid-drop dynamics.

We also performed detailed studies of the sensitivity of the control to imperfections in the shape of the geometry that generates the flow, and the variation of the velocity in the servomotors which control the position of the stagnation point. Also a detailed comparison between numeric and experimental data is also presented. This provides a complete study of the two dimensional situation. Finally, we present some open questions both in the modeling and in the theory. In particular in the possibility of extending the current results to drops of complex fluids such as viscoelastic drops, vesicles, capsules, and other immersed objects.

Given that there are no detailed studies available on the influence of the control scheme upon the drop's forms, we study numerically the influence of this control on the motion of a two dimensional drop by solving the Stokes equations in a container subjected to the appropriate boundary conditions on the cylinders and the free surface of the drop. These equations are solved with the Boundary Element Method for a variety of flows and drop parameters in order to study the perturbation effects introduced by the application of the control scheme and to provide the appropriate parameters for future experimental studies. In particular, an easy to implement control scheme is an essential tool prior to undertakings any experimental studies of the drop's dynamics -under elongational flows with vorticity at small Capillary numbers-, for large deformation of drops capsules and other objects, as well as for break up and coalescence of embedded objects.

The proposed method is simple. As the drop evolves under flow conditions, its centroid is tracked. When the drop drifts away and its centroid overtakes the prescribed domain about the nominal stagnation point, the flow is modified by adjusting the angular velocity of the cylinders according to the values obtained from the approximate solution for flows generated by TRMs. Essentially, by adjustment the angular velocities of the cylinders, the outgoing streamline environment is change into an incoming one, reversing the direction of motion of the drop, which is now towards the nominal stagnation point along a stable direction. The reversal of direction does not alter significantly the deformation rates applied upon the drop; thus, the drop's dynamics is essentially undisturbed. The process is repeated as needed and the drop is confined for long times under steady and known conditions.

This study is complementary to the previous one (Bentley 1986a, Bentley 1986b) because it allows detailed studies of the time evolution of the drop's parameters -mainly its deformation and the orientation. In contrast to FRMs, the numerical results presented allow us to study the dynamics of embedded objects under the nominal flow conditions when the drop remains at the stagnation point, as well as the drop in the “controlled flow” with the corresponding parameters. The study was carried out both under several viscosity ratios and various geometric setups, assessing the robustness of the proposed method and the very small influence it has on the drop behavior. The influence of the control scheme on the drop's parameters is small with respect to the nominal flow (around 1%). As well, the proposed control scheme is capable of relocating the stagnation point on a time scale much shorter than the time scale of the drop's evolution. Moreover, this control would remain effective during times much longer than the internal time scales for the drop evolution.

The fact that a two-dimensional numerical model for the drop is used does not compromise the results here presented, mainly because the control scheme should be applicable for small deformation of drops or for drops with very small trajectories about the stagnation point. For highly elongated drops, capsules and other complex objects, the simulated values of the drop's shape may differ from the experimental values, but the applicability of the control scheme should be equally robust.

2. Formulation of the control problem

As already demonstrated by Bentley (1986a), the only way to maintain fixed the position of the drop with respect to the flow field is by changing the location of the stagnation point via adjustments of the angular velocities of the cylinders, with the constraint that these changes must avoid significant modifications of the flow field. Consequently, a useful control scheme for flows by TRMs or FRMs has to maintain the drop as close as possible to the stagnation point for a sufficiently long time, making possible studies of the drop dynamics. From now on, the selected flow field conditions of a TRM are called nominal, and its properties such as the shear rate, flow-type parameter and the position of the stagnation point will be denoted by the subscript Nom.

Figure 1 shows the streamlines around the stagnation point of the unperturbed flow field generated by a co-rotating TRM. When a liquid or rigid particle is placed around the unstable stagnation point, the particle drifts in the direction of the outgoing streamlines. The objective of the control is to maintain a drop about the stagnation point of the nominal flow conditions. To construct the control scheme, the trajectory of the centroid of the drop is analyzed as the solution of a two dimensional dynamical system. In this case we assume that the centroid is away but near the unstable saddle point. Now if the vector field is oncoming on the boundary of a box surrounding the unstable stagnation point the system

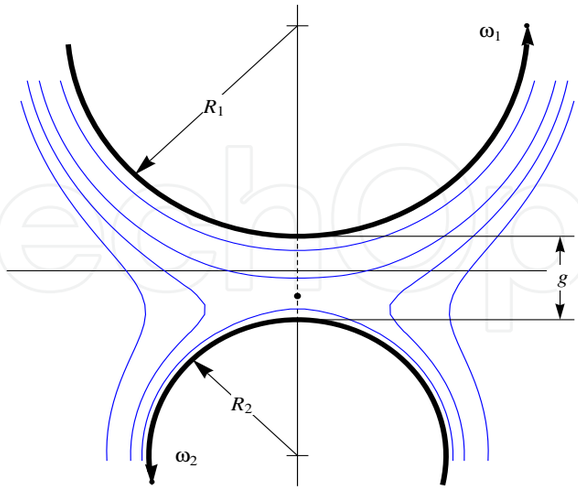

Fig. 1. Streamlines generated by a co-rotating Two-Roll Mill with different radii, showing the stagnation point in the gap between the rollers, g. The position of the stagnation point along the vertical can be moved changing the angular velocities of the rollers. The value of the flow-type parameter is a function of the position of the stagnation point.

will settle into a periodic orbit inside the box provided the vector field is time independent. When there exists time dependence, a bounded motion (which can be periodic or quasi-periodic) is produced inside the box. This motion is equally robust as the time independent case, confining the centroid of the drop to any prescribed region provided the appropriate incoming flow can be produced at the boundary.

In Fig. 2a, a rectangle is shown about the stagnation point of the flow field. The boundaries of this rectangle serve as the limits where the position of the center of mass of the fluid particle is allowed to stay at the nominal flow conditions. Fig. 2b shows a detailed sketch of the tolerance domain *PQRS* above and next to the nominal stagnation point. The dark streamlines correspond to the nominal flow field with outgoing flow exiting through the side QO_R and entering at the side RO_L of the tolerance area. The dashed flow lines which correspond to the shifted stagnation point y_{SS} with the flow field essentially reversed: the flow enters the *PQ* side and exists via *RS*. Also the flow lines which correspond to $-y_{SS}$ behave in a symmetric manner relative to the symmetric tolerance area.

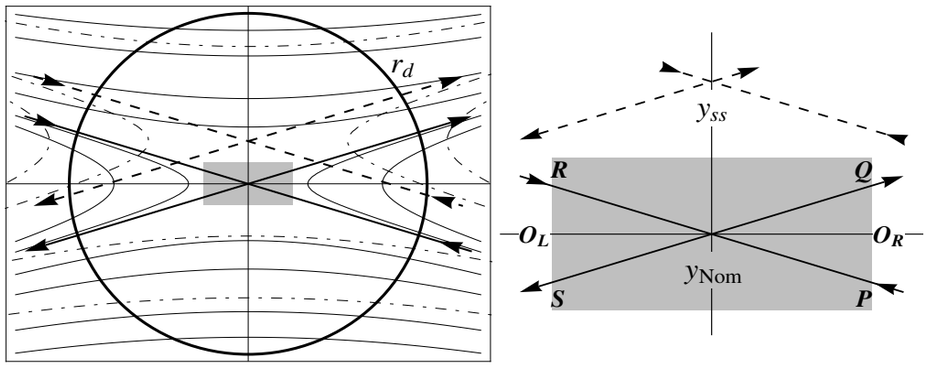

(a) (b)

Fig. 2. Streamlines around the stagnation point of the unperturbed flow field generated by a TRM.

When a fluid particle is placed around the stagnation point and the flow is started, the particle's centroid drifts away. Assume the centroid is initially at the position *A* -at time $t = 0$- located inside the tolerance area shown in Fig. 3. In this position, the flow corresponds to the nominal conditions, and the centroid is subsequently advected along the outgoing direction reaching *B* at $t = t_{on}$ when the control is applied. The control scheme effect is to displace the stagnation point to y_{SS}, switching the flow field at *B* to one towards the nominal stagnation point. As a result, the centroid follows the flow lines along the path *BC*, arriving at *C* at time $t = t_{off}$. At t_{off} the flow is reset to the nominal conditions and the stagnation point is moved back to the y_{Nom} position; thus, the centroid follows the path *CD*. At *D* the situation is repeated but now shifting the stagnation point to $-y_{SS}$ until the centroid reaches *E* where the stagnation point is shifted back to the nominal value and the centroid moves towards *F* where the process is repeated. It is to be noted that the transit time spent along paths *AB*, *CD*, *EF* is much longer that the transit time along sections *BC* and *DE* because of the small eigenvalues associated with the corresponding incoming directions which produce the motion shown. The slope of l_{in} can be modified in order to adjust the instant when the flow is reset to the nominal conditions.

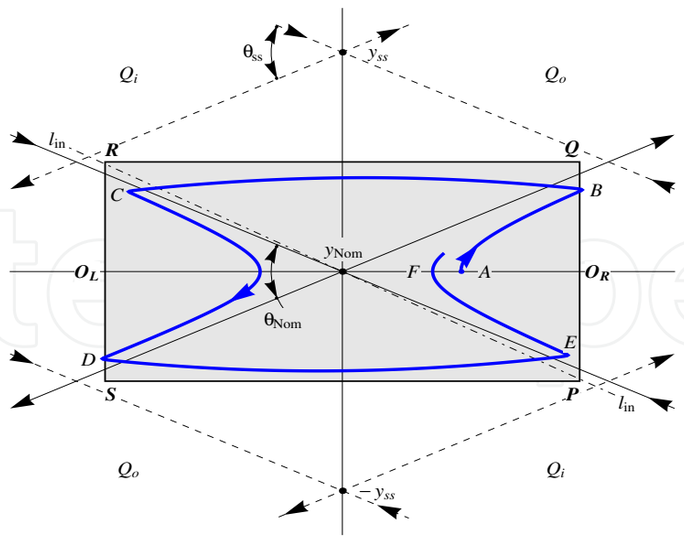

Fig. 3. Trajectory ABCDEF followed by the centroid of a fluid particle in the controlled flow field. The control area is shown in grey. The nominal flow corresponds to the darker continuous lines, and the dashed lines show the relative displacement of the flow field during the controlled portion of the cycle. The angle between the incoming and outgoing streamlines at the nominal stagnation point θ_{Nom} and the angle at the corrective flow θ_{ss} have essentially the same values.

The purpose of the implemented control scheme is to produce always an incoming flow for the drop at the boundary of the tolerance area. Thus the center of mass is effectively moved as a dynamical system with an unstable rest point (the stagnation point) but with an incoming vector field in an area surrounding the box. This arrangement guarantees the existence of an incoming vector field that provides a fixed periodic solution by the Poincaré-Bendixson theory; see Ross (1984). In this case since the incoming vector field is time dependent, a bounded trajectory is obtained that is approximately periodic. This nonlinear procedure of balancing the repulsion at the critical point with the correction of the boundary of the tolerance region always produces a very robust bounded trajectory inside any prescribed area.

All displacements of the stagnation point are assumed to be carried out on a time scale small compared to the dynamics of the drop. In the theoretical description above, both the centroid of the drop and the streamlines are adjusted instantaneously. For a laboratory experiment this will not be the case: the exact position of the centroid is determined after processing the flow field images, determining the centroid position and then the driving motors modify accordingly the flow field within a finite response time. The latter time lags are taken into account in order to calculate the effect of the control in experimental situations.

The relevant times involved are τ_1 associated to the velocity of the video system -fps- and the time of capture and processing of all images, the finite response time τ_2 of the cylinders to readjust their velocity as a consequence of the control, mainly due to the inertia of the

mechanical system, and the time of response τ_3 of the fluid around the drop to the adjustment in the velocity of the TRM. The time τ_3 of adjustment of the flow can be estimated as the diffusion time $\tau_3=l^2/\nu$ based on the gap g between the cylinders and the kinematic viscosity ν. The total response time $\tau_1 + \tau_2 + \tau_3 = \tau_c$ must be smaller than the characteristic time τ_d of the internal motion of the drop which is a function of the Capillary number and the viscosity ratio. In the present work, $\tau_1 + \tau_2 \gg \tau_3$ given the material properties of the fluids and geometry of the setup; Stokes solution implies such time scales as well.

To determine the adjusted velocity field -i.e., reposition the stagnation point position y_{SS} (or $-y_{SS}$) needed to ensure an incoming flow along PQ - a new flow line (assumed straight) is calculated, entering at PQ and ending at y_{SS}; see Fig. 3. This requirement gives y_{SS} as a function of the size of the control area. Parametrizing the flow, relating the position of the stagnation point with the angular velocities of the rollers, ω_1 and ω_2, maintaining II_{2D} constant, the required values of ω^c_1 and ω^c_2 needed to move the position of the stagnation point to y_{SS} can be calculated.

The actual control step is modeled as follows: When the centroid reaches the boundary of the tolerance area at B in Fig. 3, the angular velocities are readjusted to the calculated values ω^c_1 and ω^c_2 according to the ramp function

$$\omega^c{}_i(t) = \omega_{Nom,i} \frac{\omega^c{}_i - \omega_{Nom,i}}{2}\left(1 + tanh\left(\frac{t - t_c}{\tau_c}\right)\right) \quad (1)$$

where t_c is the time when the centroid of the particle reaches the point B, and i takes the values 1 or 2. The following step at point D is calculated in the same manner. It is remarked that during the control steps the flow parameter II_{2D} is kept constant while the change in α is less than 0.5% for all cases.

This control is different from that of Bentley and Leal. In detail, this control does not aim to stabilize the center of mass of the drop at the stagnation point as in the proportional control. The present control takes advantage of the knowledge of the local flow field and balances the unstable motion at the stagnation point with a time dependent incoming flow at the boundary, giving an effective dynamical system with a periodic or quasi-periodic orbit for the centroid. This is achieved by repositioning the velocity field; thus, producing a bounded motion inside the tolerance area as a result of a balance of instability and the modified flow. In contrast, the control by Bentley and Leal modifies the flow to project the trajectory of the centroid along the stable direction at the nominal stagnation point; essentially, a proportional method attempts to trace the centroid of the drop back to the stagnation point.

3. Experimental setup

The Two-Roll Mill experimental setup is shown in Fig. 4. The setup consists mainly of the Two-Roll Mill flow cell with controlled temperature, the driving system, the optical system and the interface system. The flow cell consist of the main body, a set of rollers of different radii with machining tolerances for cylinder's diameters and gap of less than 5 μm. The parallelism and eccentricity of the rollers axes is limited to less than 5 μm , for a top to bottom distance of 10 cm. The driving system consists of two servomotors Kollmorgen AKM-11B with

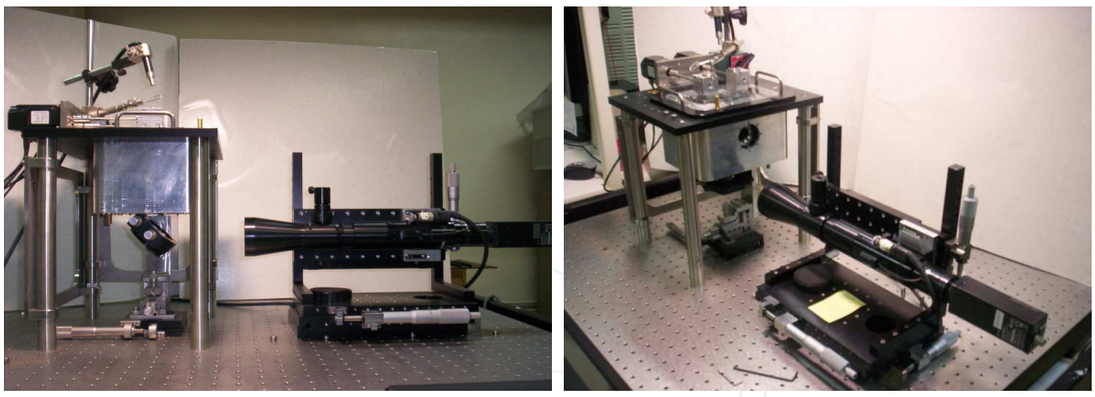

Fig. 4. Experimental setup. The flow cell with the motors and the optical system are shown.

their controllers SERCOS Servostar 300. The optical systems is made up with a Navitar microscope -with a telecentric objective with a motorized magnification of 12X-, an adapter Navitar 1-61390 with a magnification of 2X, and an IEEE 1394 CCD camera, model XCD-X700, by Sony set for a capture rate of 15 and 30 fps. The visual field is about 1.2 mm lengthwise covered with 1024 by 768 pixels. The optical resolution (based on the real part of the Optical Transfer Function) of the full assembly is about 8 μm -or better than 64 line pairs/mm. The main system is mounted on a pneumatically levitated optical workstation by Newport Research.

The typical observed response time for the computer interface, power electronics and cylinder's inertia is less than 0.01 seconds, for changes of rotational speeds less than 5% of the preset values. The flow parameters and the position of the stagnation point are adjusted by varying simultaneously the angular velocities of both cylinders ω_1 and ω_2 keeping II_{2D} constant.

Figure 5 shows a schematic block diagram of the experimental setup. A drop is initially placed near the stagnation point of the flow cell. The optical system captures images of the drop and in the computer, the shape and the center of mass is calculated, and the angular velocities of the rollers are calculated in order to maintain the drop in the position desired. The calculated angular velocities are sent to the motors controllers and a new image of the drop is captured and the cycle is repeated.

The interface system consists of a workstation HP XW4300 with a PCI SERCOS expansion card, which communicates with the motor controllers. The control software is programmed in Visual C++, in real-time mode. A Graphical User Interface (GUI) is used to provide access to the functionality of the application, see Fig. 6. It incorporates two different aspects that can be manipulated separately, one concerning to the video and the other concerning to the control of the motors.

For the video aspect, the GUI window has two displays, one is for the video input, that shows the frame that is acquired by the camera; and the other display is for the processed image, showing the contour of the drop and its center of mass, along with the tolerance area (fixed with the slide bar in the window) and the lines that corresponds to the ingoing and outgoing streamlines of the nominal stagnation point.

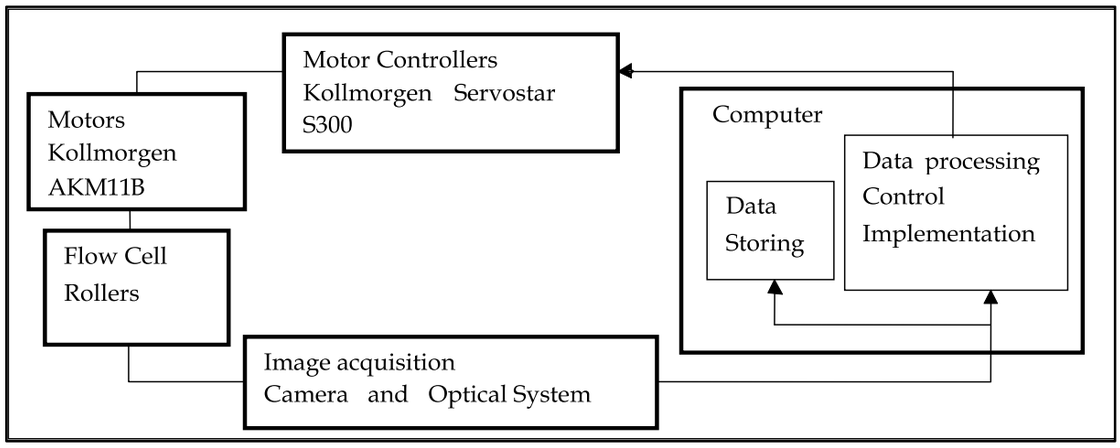

Fig. 5. Experimental block diagram.

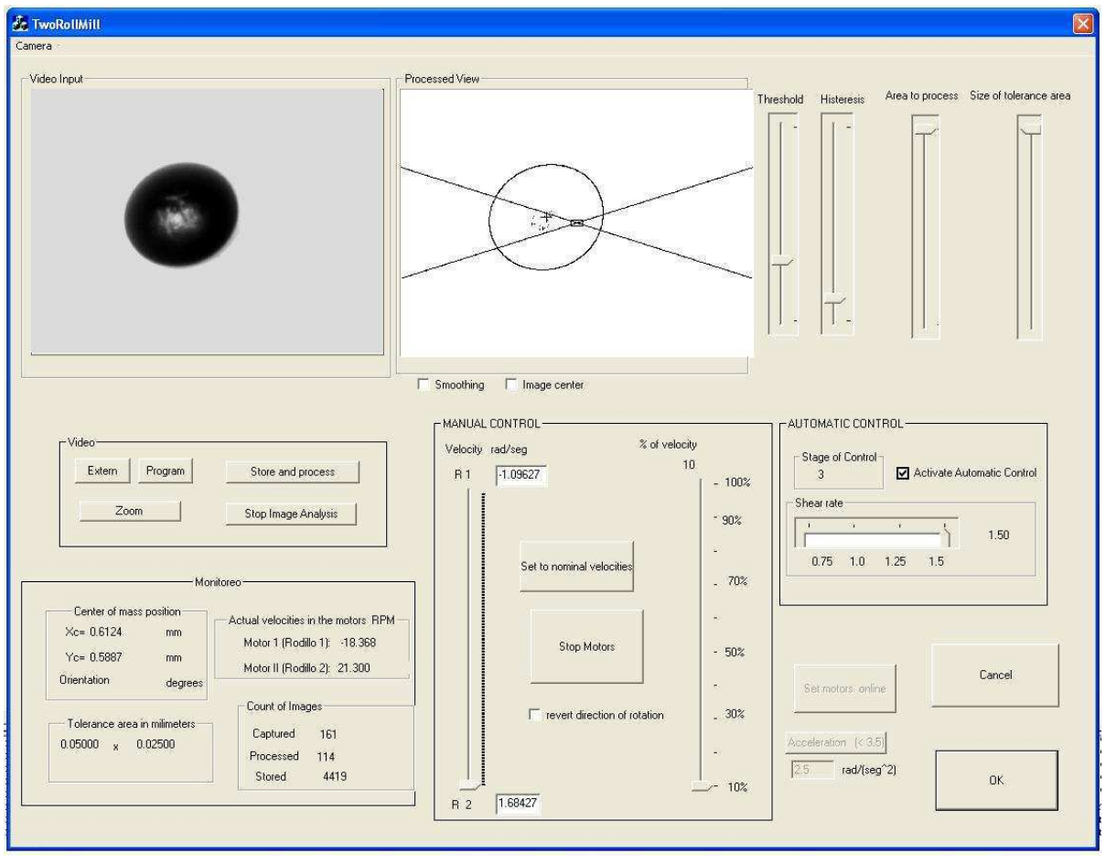

Fig. 6. Graphical User Interface (GUI) of the Two-Roll Mill Experiment.

For the control of the motors, the GUI has two parts, one is for the manual control and the other is for the automatic control. The manual control window is used for the initial positioning of the drop around the nominal stagnation point, inside the tolerance area.

For the control of the motors the window has slide bars that allow controlling the velocities of each cylinder as well as its direction of rotation. In order to place the drops in the center of the

image, it is necessary to put it in that location; this is done by manipulating its trajectory with the controls above mentioned. Once the drop is in the right place (it means the center of mass is inside the tolerance area), the automatic control is activated and the experiment goes on. The monitoring section in the window allows us to watch the instantaneous velocities of the motors, the coordinates of the center of mass and the size of the tolerance area.

4. Control scheme implementation

The automatic control for the experiment requires a real-time process. This program consists basically of three parts: (*i*) The image acquisition (*ii*) Image analysis (*iii*) Calculus and adjustment of the velocities of the motors.

4.1 Image acquisition and analysis

The images are provided by the CCD camera using the Instrumental and Industrial Digital Camera Application Programming Interface (*IIDCAPI*) by Sony in the C++ program to handle the frames provided by the camera. This section consists in two parts, the first one take the frame and stored it in a file, the second one creates a list constantly updated in order to always have the last image acquired by the camera available for the analysis section and in case of some delay in acquiring, have a reservoir of frames.

To carry out the analysis of the last frame taken, in order to find the center of mass of the drop (in pixels) we use the Open Source Computer Vision Library (OpenCV). The principal parameter is the threshold value which can be adjusted ranging from 0 to 255 in a gray-scale, used to make a binary image. In the binary image, the contour of the drop is computed using the Canny algorithm. Then the center of mass is found using the corresponding discretized integral.

4.2 Calculus and adjustment of the velocities of the motors

Is in this part where the control takes place. Once the program has the coordinates of the center of mass of the drop, decides whether is inside the tolerance area. If is not, the program calculates and modifies the velocities of the motors depending on the position of the center of mass of the drop. Also, in this part, the data of the number of the frame processed, the coordinates of the center of mass and the size of the tolerance area are stored in a file. The diagram of the control scheme is shown in Fig. 7.

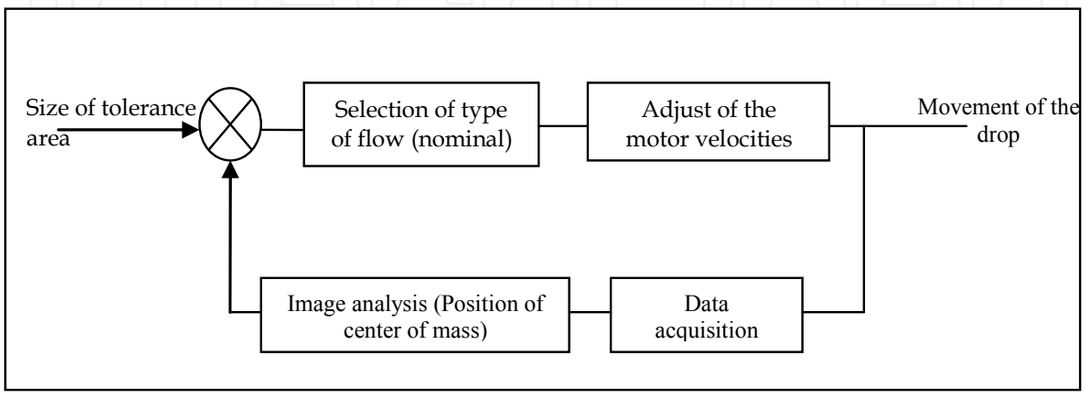

Fig. 7. Diagram of the control scheme.

5. Experimental results

5.1 Parameter used in studies of drop deformation

The parameters that govern the drop deformation and breakup are the ratio of the drop viscosity to that of the suspending fluid λ_μ, the tensorial character of $\mathbf{\nabla u}$, the history of the flow and the initial drop shape.

The Capillary number Ca represents the ratio of flow forces to surface tension, it is given by

$$Ca = \frac{a\,\dot{\gamma}\mu_1}{\Gamma} = \frac{a|\mathrm{II}_{2D}|^{1/2}\mu_1}{\Gamma} \tag{2}$$

Where II_{2D} is the second invariant of $2\mathbf{D} = \mathbf{\nabla u} + \mathbf{\nabla u}^{\mathrm{T}}$. The tensorial character of $\mathbf{\nabla u}$ gives the flow-type parameter α. For a given elongational flow with vorticity, α values close to 1 imply an elongation dominated flow, while values close to zero imply a flow with strong vorticity; that is α is a measure of the of the strength of the flow causing drops to deform, while the vorticity present in the flow induces s rotation of drops and can inhibit drop breakup. From the definition of the *flow-type parameter* α, (see Astarita, 1979),

$$\frac{1+\alpha}{1-\alpha} = \frac{\|\mathbf{D}\|}{\|\bar{\mathbf{W}}\|} \tag{3}$$

Thus α is given by

$$\alpha = \frac{\|\mathbf{D}\| - \|\bar{\mathbf{W}}\|}{\|\boldsymbol{D}\| + \|\bar{\mathbf{W}}\|} \tag{4}$$

Where $\overline{\boldsymbol{W}}$ is the objective vorticity tensor which measures the rate of rotation of a material point with respect to the rate of deformation's principal axes at that point.

A dimensionless measure of the magnitude of the drop deformation is needed. This parameter is the *Taylor Deformation Parameter* D_T, defined in terms of the longest and shortest semi-axes of the ellipsoidal drop cross section, see Fig 8.

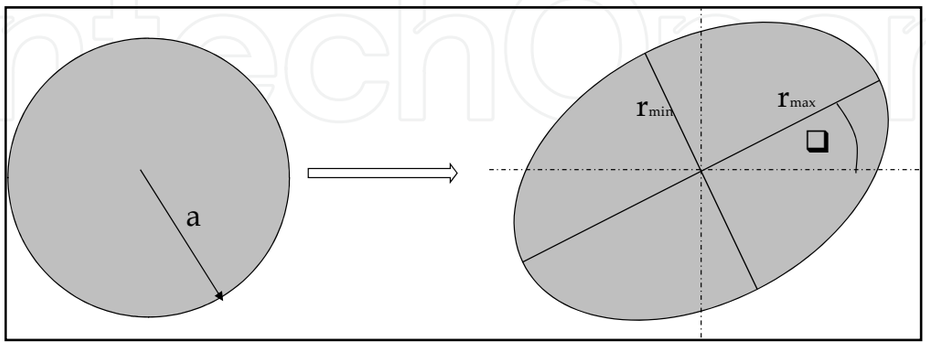

Fig. 8. Deformation Parameter DT and orientation angle.

$$\boldsymbol{D}_T = \frac{r_{max} - r_{min}}{r_{max} + r_{min}} \tag{5}$$

The orientation angle of the drop is the angle between the longest axis of the drop and the x-axis.

The flow-type parameter value is related with the angles between the incoming and the outgoing axes shown in Fig. 3 as $\theta_{Nom} = 2\,arctan\left(\sqrt{\alpha_{Nom}}\right)$ and as $\theta_{ss} = 2\,arctan\left(\sqrt{\alpha_{ss}}\right)$. In the experiment, the outgoing flow direction, about the stagnation point, is always observed responding to small differences of the refractive index of Fluid 1 due to very small differences of temperature between fluid volumes around each cylinder. Based upon reversal of the flow field -counter and co-rotating directions of the cylinders-, the angle between incoming and outgoing flow can be accurately measured within 0.1 degrees inside the visual field -less than 1.2 mm lengthwise. The observed angles are correct within ± 0.05 degrees of the nominal values here presented. This small angular uncertainty implies uncertainties for the nominal flow-type parameter of less than ± 0.5%. Thus, the experimental flow obtained is an excellent approximation for the theoretical one predicted.

The exterior fluid (Fluid 1) is a Polydimethylsiloxane oil DMS 25, η = 485 mPa s, with a relative density of 0.971. A drop (Fluid 2) of vegetable canola oil, filtered through a 3 μm pore size. At 23°C, the viscosity of Fluid 2 is η = 72.6 mPa s, with a relative density of 0.917 is used. Both liquids have a well defined Newtonian behavior at the interval of shear rate values used. The following figures show the effect on the deformation, orientation and trajectories of the centroid of a drop due to variations on the l_{in} parameter. This parameter permit adjusts the control in order to decrease the drifting effects of the τ_c time, which is a nonlinear function of the viscosity of the surrounding fluid. The drop tested had a diameter of 1.0mm, Ca = 0.1031.

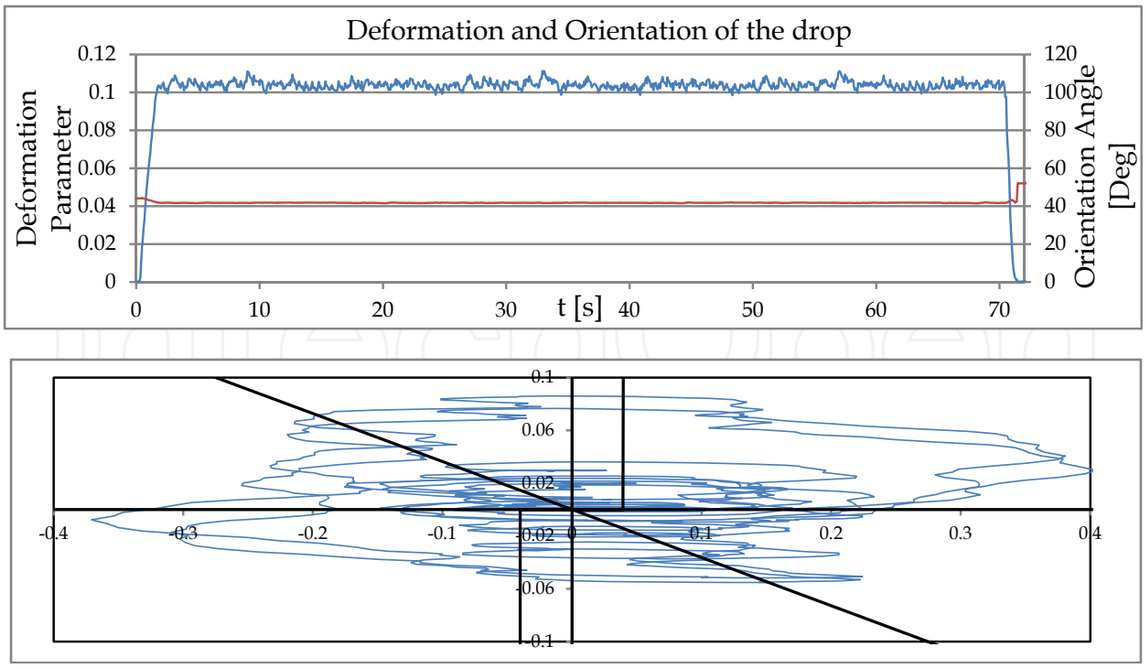

Fig. 9. Deformation, orientation and trajectory of the centroid of the drop, using the parameter l_{in} = 20°. The mean deformation is D_T = 0.1039, STD=0.002 and the mean orientation angle is 41.8°.

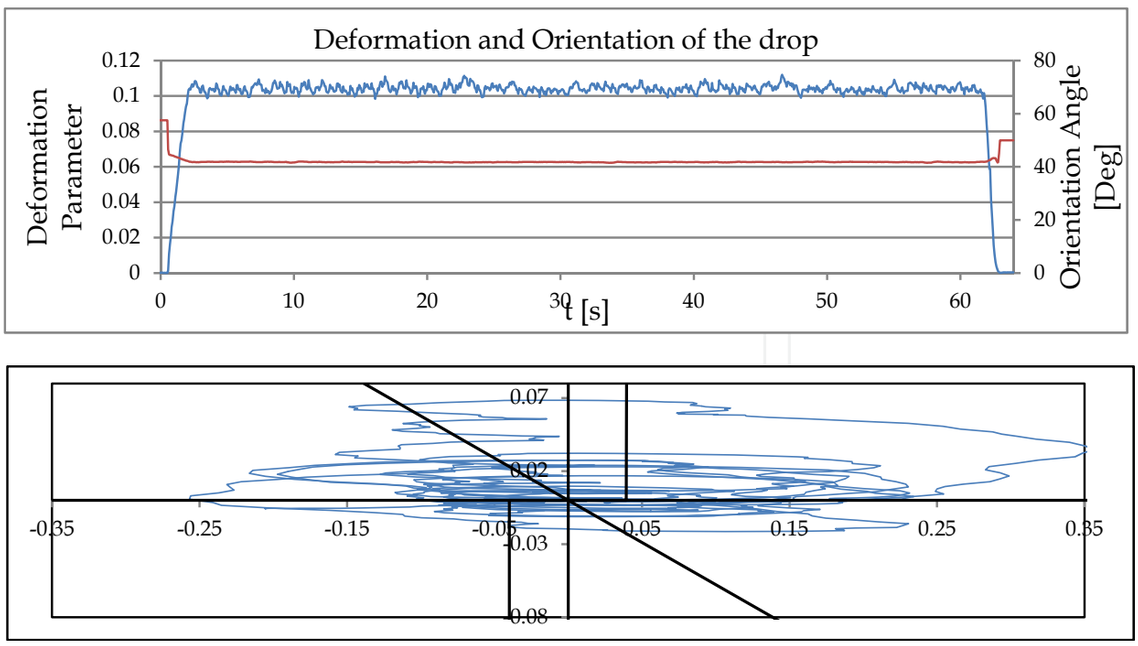

Fig. 10. Deformation, orientation and trajectory of the centroid of the drop, using the parameter $l_{in} = 30^o$. The mean deformation is $D_T = 0.1042$, STD=0.0021, the mean orientation angle is 41.8º.

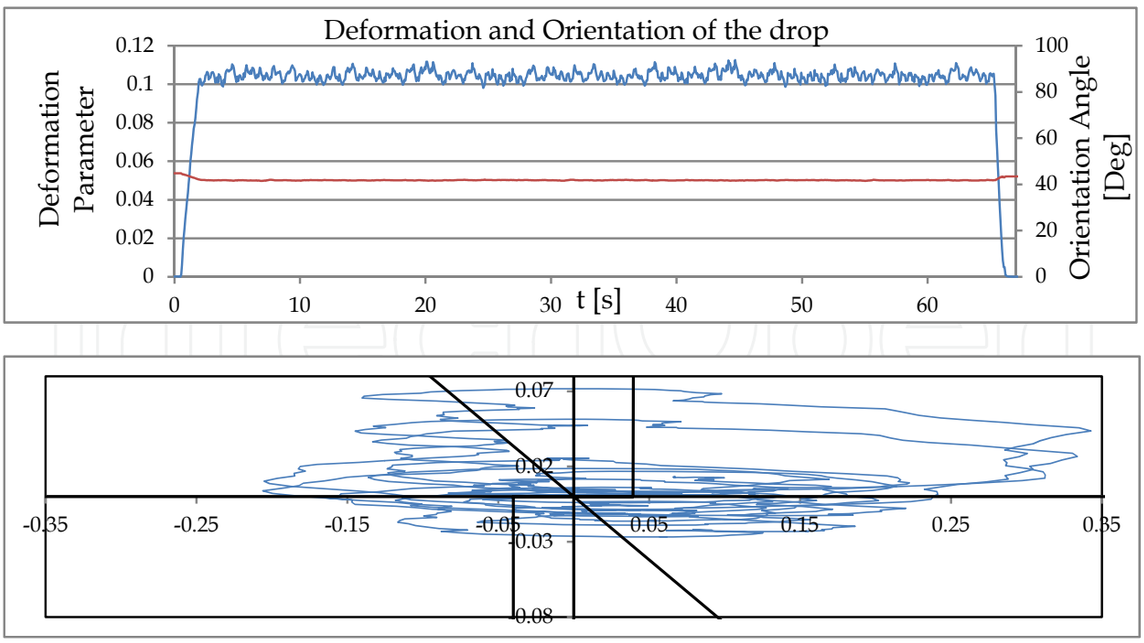

Fig. 11. Deformation, orientation and trajectory of the centroid of the drop, using the parameter $l_{in} = 40^o$. The mean deformation is $D_T = 0.1045$, STD=0.0025, and the mean orientation angle is 41.8º.

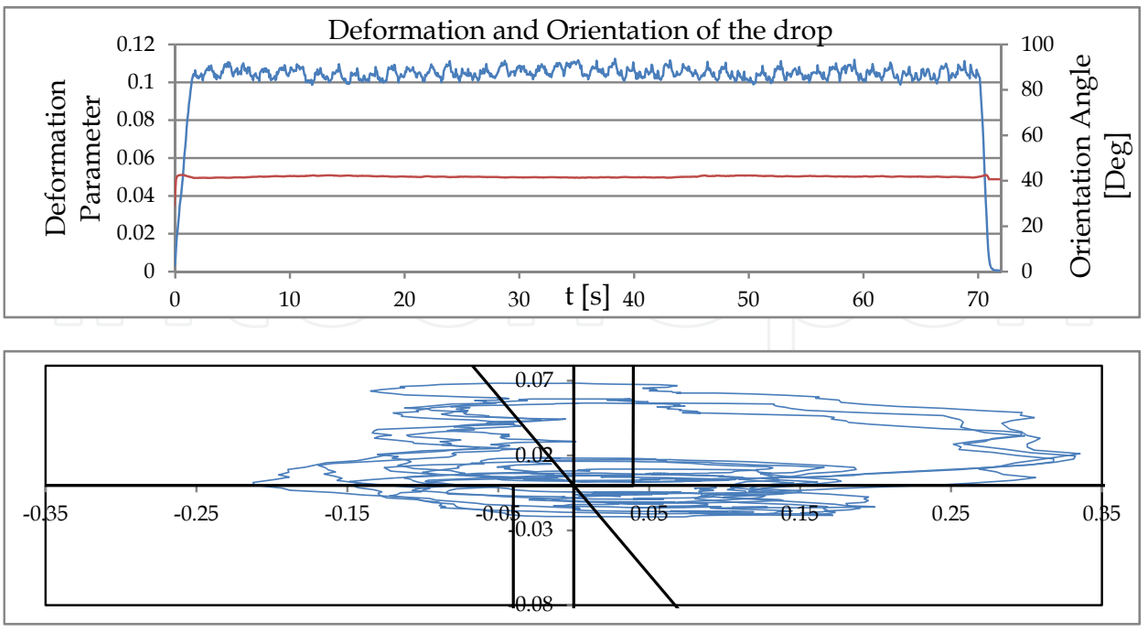

Fig. 12. Deformation, orientation and trajectory of the centroid of the drop, using the parameter l_{in} = 50º . The mean deformation is D_T = 0.1049, STD=0.0027, the mean orientation angle is 41.8º.

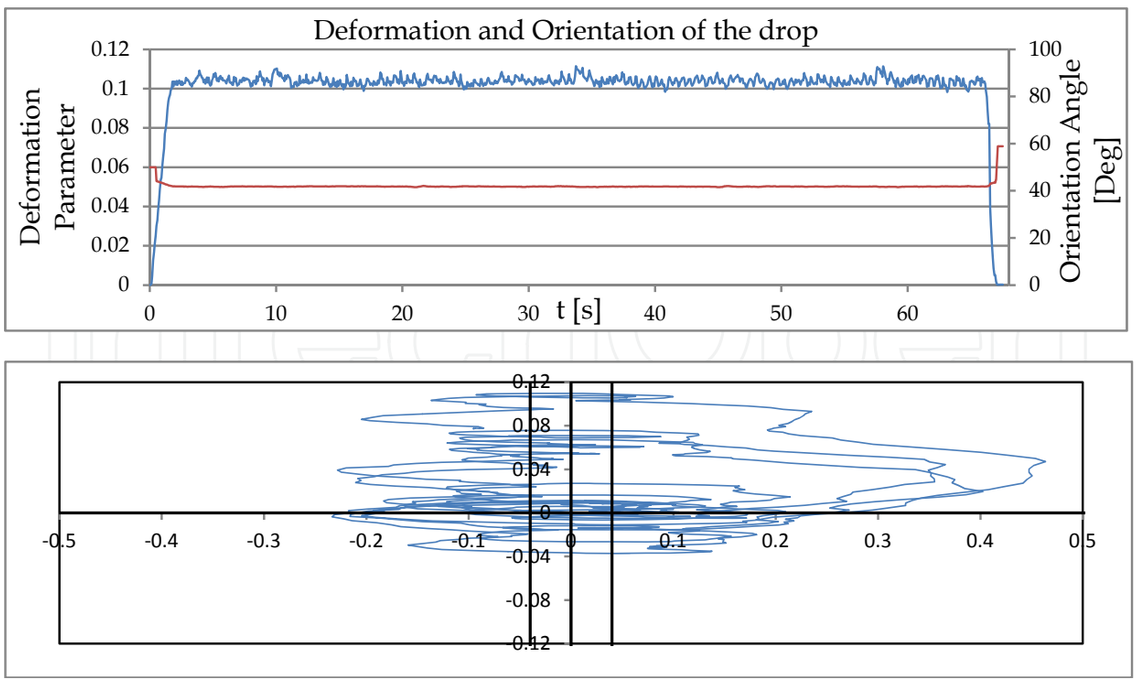

Fig. 13. Deformation, orientation and trajectory of the centroid of the drop, using vertical limits. The mean deformation is D_T = 0.1039, STD=0.0020, the mean orientation angle is 41.8º.

6. Numerical results and comparisons with the experimental results

In order to study numerically the evolution of the drop on the proposed control strategy, we use the results of Reyes *et al.* (2011). We just outline the main steps to introduce the extensions used in this Chapter to study the effect of noise and the imperfections present in the experimental situation.

We thus proceed as in Reyes *et al.* (2011) advancing the drop boundary using the equation

$$\frac{\partial \mathbf{x}}{\partial t} = (\mathbf{v}_s \cdot \mathbf{n})\mathbf{n} \tag{6}$$

where the velocity $\mathbf{v}_s$ in Eq. 6 is determined solving a boundary integral equation on the drop surface (See Pozrikidis, 1992).

The control is implemented as follows: From the new drop surface obtained from Eq. 6, we determined the center of mass of the drop using the same integral of the experiments. Once this is determined, we verified if it falls inside the tolerance region. When it is out of the selected boundary, we applied the correcting flow obtained adjusting the angular velocities using Eq. 1.

We considered the effect of noise and imperfections as follows. In the first place, we noted from the experiments a systematic variation of the angular velocity due to the geometrical imperfections of the cylinder. This was fitted with a single harmonic function with frequency and amplitude determined from the experimental values for the observed flow without drop. The random noise was taken to be white noise. With these new elements, we used the same code described in Reyes *et al.* (2011) to calculate the trajectories of the drop's center of mass, the deformation parameter and the angle of alignment in order to compare with the experimental results of the previous Section.

It is to be noted that the solution of the system are very sensitive in detail to the initial conditions. However, the broad features which depend on the limit cycle nature of the motion for the center of mass are very robust.

Because of this reason, we start the numerical solution with initial conditions for the drop's center of mass which are taken from the experimental data when the initial rapid transients have subsided. Moreover, the numerical flow is started at nominal values since the inhomogeneities presented prevent the analytical construction of the initial flow.

With this, we expect a very good agreement between the numerical and experimental values of the deformation and orientation. This is shown in Figures 14-18. Although those figures were generated with different initial conditions, the broad behavior is similar to the experimental data. The trajectories are also compared. We see good agreement in the broad features, in particular, when the control is operational.

The experimental data shows larger excursions from the nominal stagnation point. These are due to the mismatch between the commercial worm gear and worm mechanism used to reduce the angular velocity of the motors and transmit the motion to the rollers.

In Fig. 19 we display the X and Y component of the motion for the center of mass, the blue lines shows the experimental values and the red lines the numerical solution. The comparison is good considering the mismatch between the initial flows up to t = 10 s.

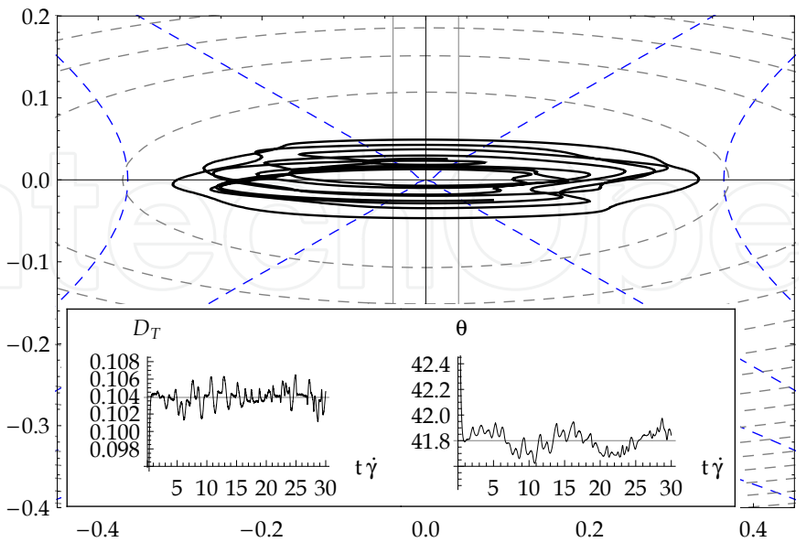

Fig. 14. Trajectory of the centroid of a drop, using vertical limits. The insert graph shows the deformation and the orientation angle. The mean deformation is D_T = 0.1039, STD = 0.000972 with a mean orientation angle of 41.8º, STD = 0.07626.

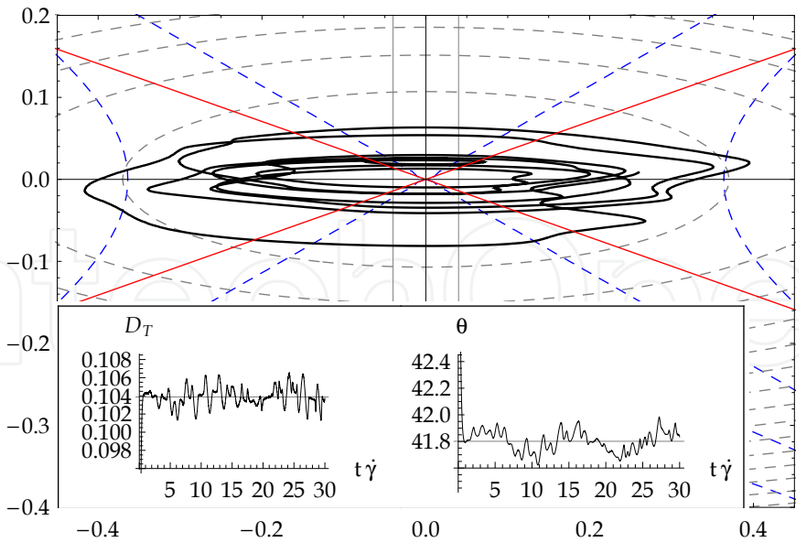

Fig. 15. Trajectory of the centroid of a drop, using the parameter l_{in} same as the incoming axis (19.435 º). The insert graph shows the deformation and the orientation angle. The mean deformation is D_T = 0.10388, STD=0.00104017 with a mean orientation angle of 41.801º, STD = 0.0764.

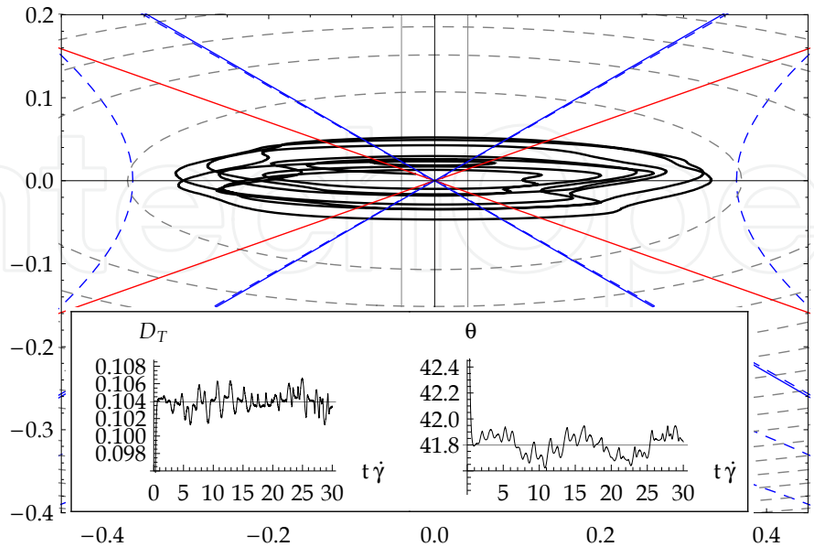

Fig. 16. Trajectory of the centroid of a drop, using the parameter l_{in} = 30 º. The insert graph shows the deformation and the orientation angle. The mean deformation is D_T = 0.103915, STD=0.0009935 with a mean orientation angle of 41.7993º, STD = 0.0784447.

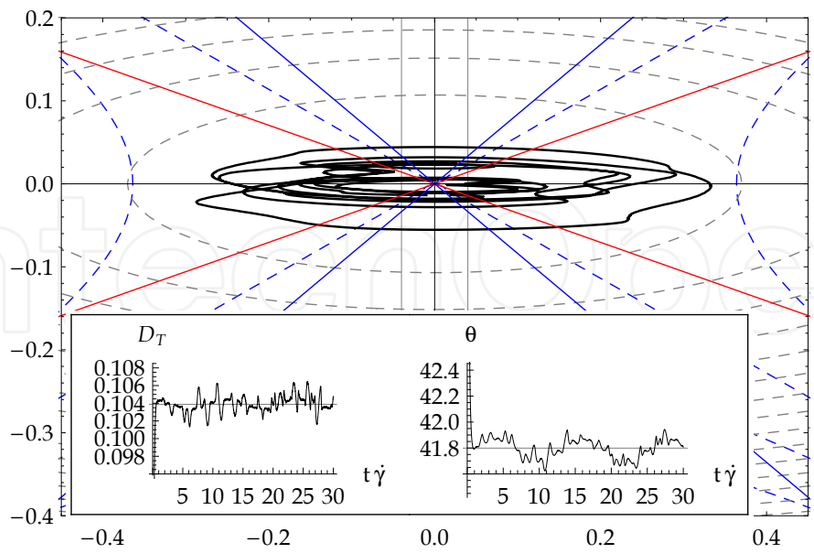

Fig. 17. Trajectory of the centroid of a drop, using the parameter l_{in} = 40 º. The insert graph shows the deformation and the orientation angle. The mean deformation is D_T = 0.103883, STD=0.00092441 with a mean orientation angle of 41.7992º, STD = 0.0735669.

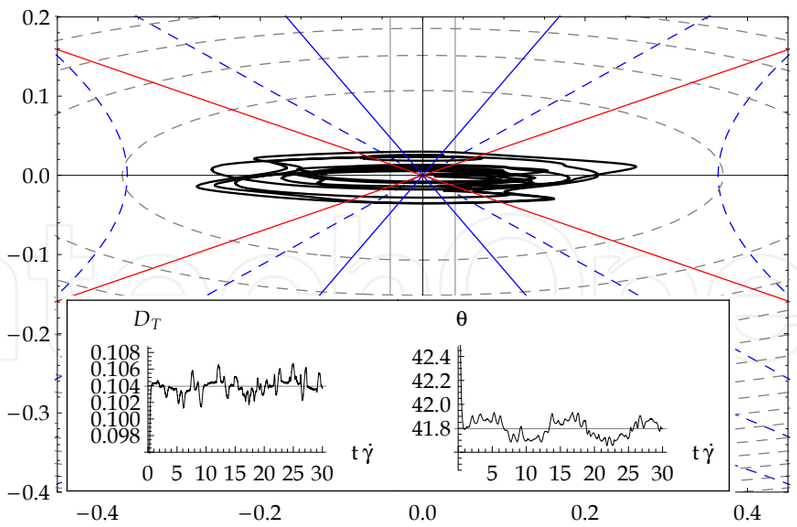

Fig. 18. Trajectory of the centroid of a drop, using the parameter l_{in} = 50°. The insert graph shows the deformation and the orientation angle. The mean deformation is D_T = 0.103934, STD=0.00096193 with a mean orientation angle of 41.7972°, STD = 0.0733545.

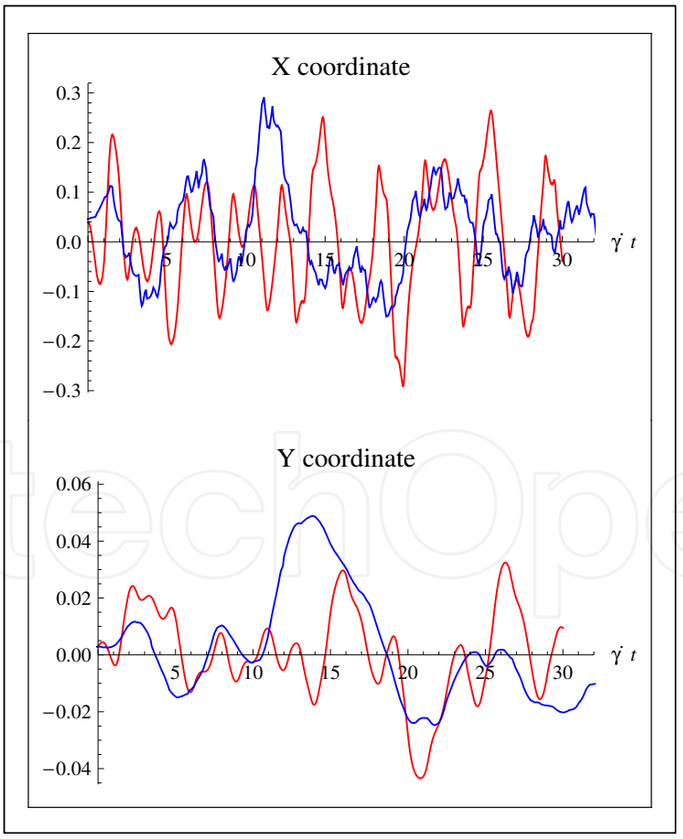

Fig. 19. Experimental and numerical comparisons of the X and Y coordinates of the center of mass of a drop subjected to the control. The blue lines are for the experimental data whereas the red lines are for the numerical data.

Beyond this time, the experimental data shows larger excursions. These are due to the mismatch between the commercial worm gear and worm mechanism used to reduce the angular velocity of the motors and transmit the motion to the rollers.

It is to be noted the remarkable agreement in the actual drop parameters which are the ones of interest.

7. Conclusions

We have shown that it is possible to maintain the position of a drop about the unstable stagnation point of the flow field generated by a TRM setup. This scheme is of the upmost importance for studies of drops in elongational flow with significant vorticity, and of relevance because its space of parameters is not accessible to FRM flows previously studied since Bentley (1986a). Indeed, TRMs expand the family of 2D elongational flows amenable with a four roll mill, albeit the former flows carry amounts of vorticity similar to that of simple shear flows.

But because the TRMs configuration can only displace the stagnation point along the line between the cylinder axes, the control scheme developed for FRMs or PBAs cannot be used for studies of drop's dynamics in elongational flows of the TRM type. For TRMs the control scheme is based upon features of Poincaré-Bendixson limiting cycles. However, these limit cycles do not imply that the wandering trajectory of the drop has to be contained in a very tight region about the nominal stagnation point. The control scheme appears capable of working for a tolerance region with the cases tested experimentally.

The control implemented in the experimental has shown to be successful. At this point, several complications have been seen in the implementation: nevertheless the control scheme is robust enough to keep the drop inside a region where the parameters of interest have a low variation, for a long times, enough to have reliable measures of the relevant parameters. The figures 9-13 shown that despite the trajectory of the drop, the parameters of interest in drop dynamics (D_T and orientation angle) are the same.

It is important to mention that even when the comparisons are made just for only one *flow-type* parameter, the results shown that it is reasonable to expect the same when we will use a different *flow-type* parameter, i.e. a different geometry.

Important differences have been observed between the experimental and numerical trajectories, this disagreement is due to mechanical imperfections, and could be fixed in the future by using an system motion transmission with better precision.

8. Acknowledgment

IYR thanks to CEP-UNAM for funding his graduate fellowship, MAHR thanks DGAPA-UNAM, AAM thanks the FENOMEC program. EG thanks CONACyT research grants.

9. References

Acrivos, A. (1983). The breakup of small drops and bubbles in shear flows. *Ann. NY Acad. Sci.*, 404:1-11

Arfken, G. (1971). *Mathematical Methods for Physicists*. 2nd Ed. Academic Press

Astarita, G. (1979). Objective and generally applicable criteria for flow classification. *Journal of Non-Newtonian Fluids Mechanics*, 6:69-76

Bentley, B. J. and L. G. Leal. (1986a). A computer-controlled four-roll mill for investigations of particle and drop dynamics in two-dimensional linear shear flows. *J. Fluid Mech.* 167:219-240

Bentley, B. J. and L. G. Leal. (1986b). An experimental investigation of drop deformation and breakup in steady two-dimensional linear flows. *J. Fluid Mech.* 167:241-283

Birkhoffer, Beat H. *et al.* (2005). Computer-controlled flow cell for the study of particle and drop dynamics in shear flow fields. *Ind. Eng. Chem. Res.* 44:6999-7009

Geffroy E. and L. G. Leal. (1992). Flow Birefringence of a Concentrated Polystyrene Solution in a Two Roll-Mill 1. Steady Flow and Start-Up of Steady Flow. *J. Polym. Sci. B: Polym. Phys.* 30(12):1329-1349

Gradshteyn, I. S. and I. M. Ryzhik. (1981). *Tables of integrals, series and products*. Academic Press

Jeffery, G. B. (1922). The rotation of two circular cylinders in a viscous fluid. *Proc Royal Society A* 101:169-174

Pozrikidis, C. (1992). *Boundary Integral and singularity methods for linearized viscous flow*. Cambridge University Press

Pozrikidis, C. (2003). *Modeling and simulation of capsules and biological cells*. CRC Press

Rallison J. M. (1980). A note of the time-dependent deformation of a viscous drop which is almost spherical. *J. Fluid Mechanics* 98(3):625-633

Reyes, M. A. H. and E. Geffroy. (2000). Study of low Reynolds number hydrodynamics generated by symmetric co-rotating two-roll mills. *Revista Mexicana de Física* 46(2):135-147

Reyes, M. A. H. and E. Geffroy. (2000). A co-rotating two-roll mill for studies of two-dimensional, elongational flows with vorticity. *Phys. Fluids* 12(10):2372-2376.

Reyes, M. A. H., A. A. Minzoni & E. Geffroy (2011), Numerical study of the effect of nonlinear control on the behavior of a liquid drop in elongational flow with vorticity", *Journal of Engineering Mathematics,* 71(2):185-203.

Ross, S. (1984). *Differential Equations*. Wiley

Singh, P. and L. G. Leal. (1994). Computational studies of the FENE dumbbell model in a co-rotating two-roll mill. *J. Rheol.* 38:485-517

Stone, H. A. (1994). Dynamics of drop deformation and breakup in viscous fluids. *Ann. Rev. Fluid Mech.* 26:65-102

Taylor, G. I. (1932). The Viscosity of a Fluid Containing Small Drops of Another Fluid. *Proc. R. Soc. London*, Ser. A, 138:41-48

Taylor, G. I. (1934). The Formation of Emulsions in Definable Fields of Flow. *Proc. R. Soc. London*, Ser. A 146:501-523

Torza S., R. G. Cox and S. G. Mason. (1972). Particle motions in shear suspensions. *J. Colloid and Interface Sci.* 38(2):395-411

Wang, J. J., D. Yavich, and L. G. Leal. (1994). Time resolved velocity gradient and optical anisotropy in lineal flow by photon correlation spectroscopy. *Phys. Fluids* 6(11):3519-3534

Yang, H., C. C. Park, Y. T. Hu, and L. G. Leal. (2001). The coalescence of two equal--sized drops in a two dimensional linear flow. *Phys. Fluids* 13(5):1087-1106

Applications of Nonlinear Control

Edited by Dr. Meral Altınay

ISBN 978-953-51-0656-2
Hard cover, 202 pages
Publisher InTech
Published online 13, June, 2012
Published in print edition June, 2012

A trend of inverstigation of Nonlinear Control Systems has been present over the last few decades. As a result the methods for its analysis and design have improved rapidly. This book includes nonlinear design topics such as Feedback Linearization, Lyapunov Based Control, Adaptive Control, Optimal Control and Robust Control. All chapters discuss different applications that are basically independent of each other. The book will provide the reader with information on modern control techniques and results which cover a very wide application area. Each chapter attempts to demonstrate how one would apply these techniques to real-world systems through both simulations and experimental settings.

How to reference

In order to correctly reference this scholarly work, feel free to copy and paste the following:

Israel Y. Rosas, Marco A. H. Reyes, A. A. Minzoni and E. Geffroy (2012). Nonlinear Control Applied to the Rheology of Drops in Elongational Flows with Vorticity, Applications of Nonlinear Control, Dr. Meral Altınay (Ed.), ISBN: 978-953-51-0656-2, InTech, Available from: http://www.intechopen.com/books/applications-of-nonlinear-control/nonlinear-control-applied-to-the-rheology-of-drops-in-elongational-flows-with-vorticity

INTECH
open science | open minds

InTech Europe
University Campus STeP Ri
Slavka Krautzeka 83/A
51000 Rijeka, Croatia
Phone: +385 (51) 770 447
Fax: +385 (51) 686 166
www.intechopen.com

InTech China
Unit 405, Office Block, Hotel Equatorial Shanghai
No.65, Yan An Road (West), Shanghai, 200040, China
中国上海市延安西路65号上海国际贵都大饭店办公楼405单元
Phone: +86-21-62489820
Fax: +86-21-62489821

IntechOpen